

Hard exclusive π^+n electro production beam spin asymmetries off the proton in the GPD and TDA regimes

S. Diehl^{1,2*} for the CLAS collaboration

¹ II. Physikalisches Institut der Universität Gießen, 35392 Gießen, Germany

² University of Connecticut, Storrs, Connecticut 06269, USA

* stefan.diehl@exp2.physik.uni-giessen.de

June 2, 2021

1 Abstract

Hard exclusive π^+n electro-production can be used to gain access to the 3D nucleon structure. The QCD factorisation mechanism in the "nearly forward region" (t/Q^2 small) allows a description by Generalized Parton Distributions (GPDs), while for the "nearly backward" kinematic region (u/Q^2 small) a description based on nucleon to pion transitions (TDAs) is available. The paper presents a measurement of single beam spin asymmetries to extract the $A_{LU}^{\sin\phi}$ moments and the related cross section ratio $\sigma_{LT'}/\sigma_0$ from the hard exclusive π^+ channel off the unpolarized hydrogen target in a wide range of kinematics based on data taken with the CLAS spectrometer at Jefferson Lab. In addition, under forward angles a detailed multidimensional study will be presented based on CLAS12 data and compared to theoretical predictions.

13 1 Introduction

Hard exclusive pseudoscalar meson production can be used to study the 3D nucleon structure in terms of the transverse position and the longitudinal momentum component. Applying QCD factorisation, the process in the "nearly forward region" (t/Q^2 small) can be divided into a hard part, described by perturbative QCD and in two general structure functions, the Generalized Parton Distributions (GPDs) for the nucleon and the pion distribution amplitudes (DAs), describing the complex non perturbative structure of these particles [1–3]. Depending on the polarisation of the quarks and the nucleon, there are in total eight GPDs, of which four are chiral-even and four chiral-odd. While the chiral-even GPDs (H , \tilde{H} , E and \tilde{E}) can be well accessed by deeply virtual Compton scattering (DVCS), pseudoscalar meson production can be used to probe also the chiral-odd GPDs (H_T , \tilde{H}_T , E_T , and \tilde{E}_T) [4–6].

In the "nearly backward" kinematic region (u/Q^2 small) a collinear factorized description in terms of a convolution of the non-perturbative nucleon to pion transitions (TDAs), the nucleon DAs and the hard interaction amplitude from pQCD is assumed to be valid [7–10]. Nucleon-to-meson TDAs are universal functions that parametrize the non-perturbative structure of these hadrons. Within the TDA mechanism, the three-quark core of the target nucleon absorbs most of the virtual photon momentum and recoils forward, while a low momentum pion is emitted under backward angles. This process allows us to get new insights into the hadronic structure and to probe non-minimal Fock components of hadronic light-cone wave functions. Recent publications on exclusive π^+ electro-production [11] and on ω electro-production [12] in backward kinematics, provided first indications for the applicability of the TDA mechanism.

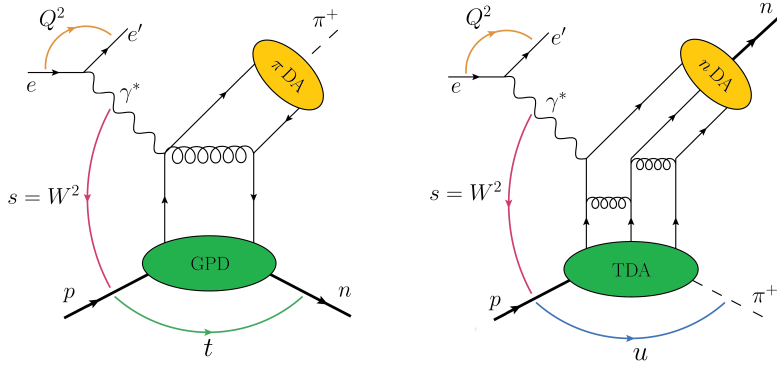


Figure 1: Left: Diagram of the GPD mechanism in very forward kinematics ($-t/Q^2 \ll 1$). Right: Diagram of the TDA mechanism in very backward kinematics ($-u/Q^2 \ll 1$). [13]

36 The reaction mechanisms in the GPD and TDA regimes are compared in Fig. 1.

37 For exclusive meson production, GPDs and TDAs can be accessed through different
 38 observables, such as differential cross sections and beam and target polarization asymme-
 39 tries [14, 15]. The focus of this work is on the extraction of the $A_{LU}^{\sin \phi}$ moment and the
 40 related cross section ratio $\sigma_{LT'}/\sigma_0$ from beam-spin asymmetries. According to [14], the
 41 beam-spin asymmetry can be defined as:

$$BSA(t, \phi, x_B, Q^2) = \frac{d\sigma^+ - d\sigma^-}{d\sigma^+ + d\sigma^-} = \frac{A_{LU}^{\sin \phi} \sin \phi}{1 + A_{UU}^{\cos \phi} \cos \phi + A_{UU}^{\cos 2\phi} \cos 2\phi}, \quad (1)$$

42 where $d\sigma^\pm$ is the differential cross section for the two beam helicity states (\pm). The
 43 subscripts ij represent the longitudinal (L) or unpolarized (U) state of the beam and
 44 the target and ϕ is the azimuthal angle between the electron scattering and the hadron
 45 production plane. The moments $A_{LU}^{\sin \phi}$, $A_{UU}^{\cos \phi}$ and $A_{UU}^{\cos 2\phi}$ can be directly related to the
 46 ratio of the interference cross sections $\sigma_{LT'}$, σ_{LT} , σ_{TT} and the non ϕ dependent part of
 47 the cross section $\sigma_0 = \sigma_T + \epsilon\sigma_L$ [16]:

$$A_{LU}^{\sin \phi} = \sqrt{2\epsilon(1-\epsilon)} \frac{\sigma_{LT'}}{\sigma_0}, \quad A_{UU}^{\cos \phi} = \sqrt{2\epsilon(1+\epsilon)} \frac{\sigma_{LT}}{\sigma_0}, \quad A_{UU}^{\cos 2\phi} = \epsilon \frac{\sigma_{TT}}{\sigma_0} \quad (2)$$

48 where the structure functions σ_L and σ_T correspond to transverse (T) and longitudinal
 49 (L) polarized virtual photons. The ratio of their fluxes is given by ϵ , which is determined
 50 by the electron scattering kinematics.

51 The Golskokov-Kroll (GK) model [17] can be used to describe $\sigma_{LT'}$ in terms of GPDs.
 52 The model includes chiral-odd GPDs to calculate the contributions from the transversely
 53 polarized virtual photon amplitudes [17]. The GPDs are constructed from double distri-
 54 butions and constrained by results from lattice QCD and transversity parton distribution
 55 functions [17]. The pion pole contribution to the amplitudes is taken into account. An
 56 expression for $\sigma_{LT'}$ is provided through the convolutions of GPDs with sub-process ampli-
 57 tudes (see Fig. 1 left) and contains the products of chiral-odd and chiral-even GPDs [4]:
 58 $\sigma_{LT'} \sim \text{Im} \left[\langle \bar{E}_T \rangle^* \langle \tilde{H} \rangle + \langle H_T \rangle^* \langle \tilde{E} \rangle \right]$, where all involved GPDs are influenced directly or
 59 indirectly by the pion pole term (i.e. $\tilde{E}_{eff} = \tilde{E} + \text{pole}$), which significantly amplifies
 60 the imaginary part of small chiral-odd GPDs in the case of π^+ [13]. Due to the quark
 61 composition of π^+ and the resulting wave function, it can be also assumed that $\langle \bar{E}_T \rangle$ is
 62 small. Therefore, $\sigma_{LT'}$ is dominated by $\text{Im}[\langle H_T \rangle^* \langle \tilde{E} \rangle]$ for π^+ .

63 In the backward regime a similar expression of $\sigma_{LT'}$ can be found within the TDA
 64 model through the interference between the leading twist transverse amplitude of the
 65 convolution in terms of twist-3 πN TDAs and nucleon DAs and the next leading sub-
 66 process longitudinal amplitude of the convolution involving twist-4 TDAs and DAs [13].
 67 However, a complete theoretical study of this twist-4 longitudinal amplitude is not yet
 68 available.

69 2 Extraction of beam spin asymmetries over a wide range 70 of kinematics with CLAS

71 A first study of hard exclusive π^+ electro-production beam spin asymmetry over a wide
 72 range of kinematics, was performed at Jefferson Lab with the CEBAF Large Acceptance
 73 Spectrometer (CLAS) [18]. This work is published in Ref. [13]. The study used a longitudi-
 74 nally polarized electron beam with an energy of 5.498 GeV interacting with a unpolarized
 75 liquid hydrogen target. For the selection of deeply inelastic scattered electrons, cuts on
 76 $Q^2 > 1 \text{ GeV}^2$ and on the invariant mass of the hadronic final state $W > 2 \text{ GeV}$ were
 77 applied. The exclusive $e'\pi^+n$ final state, was selected from the detected electrons and π^+
 78 by a cut around the neutron peak in the $e\pi^+X$ missing mass spectrum.

79 Experimentally the BSA and its statistical uncertainty are defined with the number of
 80 counts with positive and negative helicity (N_i^\pm), in a specific bin i as:

$$BSA = \frac{1}{P_b} \frac{N_i^+ - N_i^-}{N_i^+ + N_i^-}, \quad \sigma_{BSA} = \frac{2}{P_b} \sqrt{\frac{N_i^+ N_i^-}{(N_i^+ + N_i^-)^3}}, \quad (3)$$

81 where $P_b = 74.9 \pm 2.4\%$ (stat.) $\pm 3.0\%$ (sys.) is the magnitude of the beam polariza-
 82 tion. A fit to the ϕ dependence of the BSA, following Eq. (1) was applied to extract
 83 the $A_{LU}^{\sin\phi}$ moment. The asymmetry of the background has been subtracted on a bin by
 84 bin basis. Several sources of systematic uncertainty were investigated, including particle
 85 identification, background subtraction, beam polarization, and the influence of the $A_{UU}^{\cos\phi}$
 86 and $A_{UU}^{\cos 2\phi}$ moments. The impact of acceptance effects was estimated based on Monte
 87 Carlo simulations. More details can be found in Ref. [13].

88 $A_{LU}^{\sin\phi}$ was extracted over the complete range of $-t$ up to 6.6 GeV^2 as shown in Fig. 2,
 89 which is close to the maximal accessible $-t$ value. The data is integrated over Q^2 , ranging
 90 from $1 \text{ GeV}^2 - 4.5 \text{ GeV}^2$ and x_B ranging from 0.1 to 0.6. Fig. 2 clearly shows, that
 91 the t -dependence of $A_{LU}^{\sin\phi}$ makes a transition from positive values in the forward region
 92 (small $-t$) to negative values in the backward region (large $-t$, small $-u$) [13]. The sign
 93 change occurs around $-t = 3 \text{ GeV}^2$, which corresponds to 90 degrees in the center of mass
 94 frame, and marks the transition between the π^+ emitted in the forward and backward
 95 directions. Therefore, the sign change may indicate a transition between the GPD and
 96 TDA regimes [13]. Additional studies showed, that the sign change occurs in the complete
 97 accessible Q^2 and x_B region [13].

99 3 A multidimensional study in the GPD regime with CLAS12

100 Based on the new CLAS12 (CEBAF Large Acceptance Spectrometer for experiments at
 101 12 GeV) [19] data, a detailed multidimensional study of $\sigma_{LT'}/\sigma_0$ has been performed in
 102 the GPD regime. The experiment uses a longitudinally polarized electron beam, with an

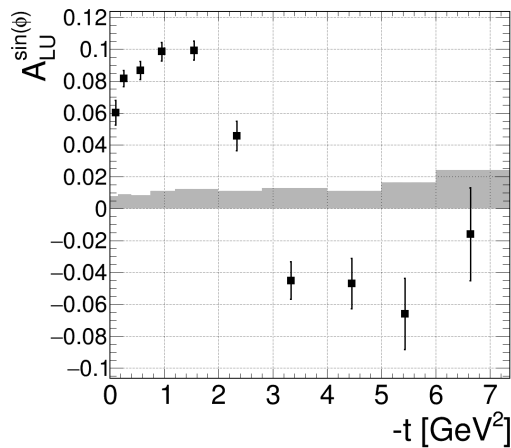


Figure 2: $A_{LU}^{\sin\phi}$ as function of $-t$. The shaded area represents the systematic uncertainty of the measurement. The figure is taken from [13].

103 energy of 10.6 GeV, interacting with an unpolarized liquid hydrogen target. The CLAS12
 104 forward detector consists of six identical sectors within a toroidal magnetic field. The
 105 momentum and the charge of the particles were determined by 3 regions of drift cham-
 106 bers. The electron identification was based on a lead-scintillator electromagnetic sampling
 107 calorimeter in combination with a Cherenkov counter. Positive pions were identified by
 108 time-of-flight measurements. Cuts on $Q^2 > 1 \text{ GeV}^2$ and $W > 2 \text{ GeV}$ were applied. The
 109 exclusive $e'\pi^+n$ events are selected from the detected electron and π^+ by a cut around the
 110 neutron peak in the $e\pi^+X$ missing mass spectrum and the background is subtracted on a
 111 bin by bin basis.

112 Figure 3 shows the Q^2 vs x_B distribution and the applied binning scheme for these
 variables. The extraction of the beam spin asymmetry follows the methods described for

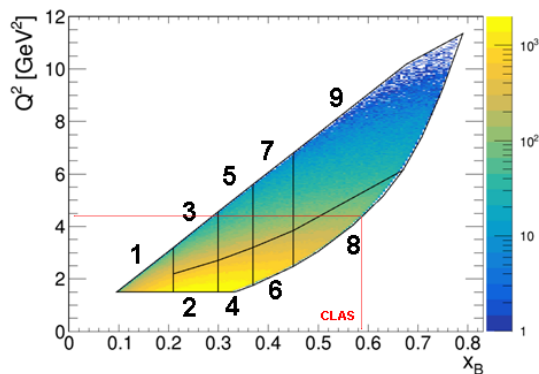


Figure 3: Q^2 vs x_B distribution accessible with CLAS12. The black lines and the numbers indicate the binning scheme used for the multidimensional study. The red line illustrates the region which was accessible with CLAS.

113
 114 CLAS in section 2. The results for $\sigma_{LT'}/\sigma_0$ in the region of $-t$ up to 1.2 GeV^2 ($-t/Q^2 \ll 1$),
 115 where the leading-twist GPD framework is applicable are shown in Fig. 4. The theoretical
 116 predictions from the GPD-based model by Goloskokov and Kroll [17] are shown as a blue
 117 line. The multidimensional study allows a more detailed investigation of the Q^2 and x_B
 118 dependence of $\sigma_{LT'}/\sigma_0$ and a precise comparison to the theory predictions in the different
 119 kinematic regions. The comparison with predictions from the GPD based GK model [17]
 120 shows, that while the magnitude is overestimated by the model, the general slope of the t -

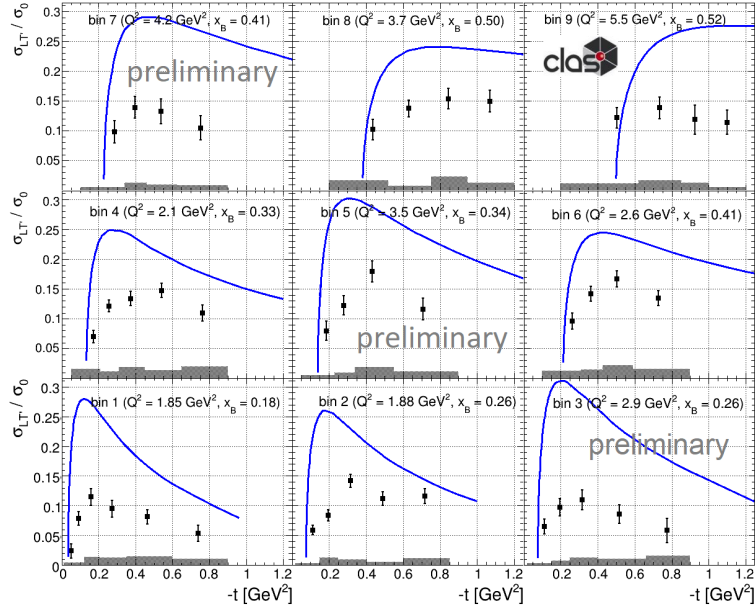


Figure 4: $\sigma_{LT'}/\sigma_0$ as function of $-t$ for different $Q^2 - x_B$ bins according to the binning scheme shown in Fig. 3. The gray histogram shows a preliminary estimate of the systematic uncertainty. The blue line shows the predictions from the GK model [17] at the stated mean value of the bins kinematics.

121 dependence and its variation between the single $Q^2 - x_B$ bins shows a similar but especially
 122 at low Q^2 not fully identical behavior between the model and the experimental results.
 123 The mismatch of the amplitude can be interpreted as an indication for an underestimated
 124 magnitude of the so far poorly known GPD H_T which is amplified by the interplay with
 125 the pion pole term.

126 4 Conclusion

127 In summary, the initial study based on CLAS data, provided an extraction of $A_{LU}^{\sin\phi}$ for
 128 $\vec{e}p \rightarrow e'n\pi^+$ at large photon virtuality, above the resonance region over the full range of
 129 kinematics in $-t$, covering the complete kinematic region of the GPD and TDA frameworks
 130 simultaneously. A clear sign change of $A_{LU}^{\sin\phi}$ has been observed, indicating a transition
 131 from the GPD to the TDA regime. This data-set will help to develop reaction mechanisms
 132 for a description of the full kinematic region. Based on the new CLAS12 data it became
 133 possible for the first time to do a more detailed multidimensional study of $\sigma_{LT'}/\sigma_0$ in the
 134 GPD regime, which allowed an investigation of the Q^2 and x_B dependence of the results.
 135 A comparison with predictions from the GPD based GK model [17] showed, that while
 136 the magnitude is overestimated, the general slope of the t -dependence and its variation in
 137 the single $Q^2 - x_B$ bins shows a similar but not fully identical behavior in experiment and
 138 theory. The mismatch of the amplitude can be seen as an indication for an underestimated
 139 magnitude of the so far poorly known GPD H_T . In combination with previous and future
 140 cross section measurements and results from the π^0 and η channels, the presented data will
 141 help to better constrain this poorly known GPD in an extended kinematic range. Once
 142 more data becomes available from CLAS12 detailed multidimensional studies of the TDA
 143 regime will follow.

144 Acknowledgements

145 We acknowledge the outstanding efforts of the staff of the Accelerator and the Physics
146 Divisions at Jefferson Lab in making this experiment possible. The authors want to
147 thank P. Kroll, B. Pire, K. Semenov-Tian-Shansky and L. Szymanowski for many fruitful
148 discussions concerning the interpretation of our results.

149 **Funding information** This work was supported in part by the U.S. Department of En-
150 ergy, the National Science Foundation (NSF), the Italian Istituto Nazionale di Fisica Nucle-
151 are (INFN), the French Centre National de la Recherche Scientifique (CNRS), the French
152 Commissariat pour l’Energie Atomique, the UK Science and Technology Facilities Council,
153 the National Research Foundation (NRF) of Korea, the Helmholtz-Forschungsakademie
154 Hessen für FAIR (HFHF) and the Ministry of Science and Higher Education of the Rus-
155 sian Federation. The Southeastern Universities Research Association (SURA) operates
156 the Thomas Jefferson National Accelerator Facility for the U.S. Department of Energy
157 under Contract No. DE-AC05-06OR23177.

158 References

- 159 [1] D. Müller et al., Fortsch. Phys. **42**, 101 (1994).
160 [2] A. V. Radyushkin, Phys. Lett. B **380**, 417 (1996).
161 [3] X. Ji, Phys. Rev. Lett. **78**, 610 (1997).
162 [4] S. V. Goloskokov and P. Kroll, Eur. Phys. J. A **47**, 112 (2011).
163 [5] G. R. Goldstein, J. O. Hernandez and S. Liuti, Phys. Rev. D **91**, 114013 (2015).
164 [6] M. Diehl and W. Kugler, Eur. Phys. J. C **52**, 933 (2007).
165 [7] L. L. Frankfurt, P. V. Pobylitsa, M. V. Polyakov and M. Strikman, Phys. Rev. D **60**,
166 014010 (1999).
167 [8] B. Pire and L. Szymanowski, Phys. Lett. B **622**, 83 (2005).
168 [9] B. Pire and L. Szymanowski, Phys. Rev. D **71**, 111501(R) (2005).
169 [10] J. P. Lansberg, B. Pire and L. Szymanowski, Phys. Rev. D **75**, 074004 (2007).
170 [11] K. Park et al. (*CLAS Collaboration*), Phys. Lett. B **780**, 340 (2018).
171 [12] W. B. Li et al. (*Jefferson Lab F_π Collaboration*), Phys. Rev. Lett. **123**, 182501 (2019).
172 [13] S. Diehl et al. (*CLAS Collaboration*), Phys. Rev. Lett. **125**, 182001 (2020).
173 [14] D. Drechsel and L. Tiator, J. Phys. G **18**, 449 (1992).
174 [15] M. Diehl and S. Sapeta, Eur. Phys. J. C **41**, 515 (2005).
175 [16] Arens, O. Nachtmann, M. Diehl, P. V. Landshoff, Z.Phys. C **74**, 651 (1997).
176 [17] S. V. Goloskokov and P. Kroll, Eur. Phys. J. C **65**, 137 (2010).
177 [18] B. A. Mecking et al. (*CLAS Collaboration*), Nucl. Instr. Meth. A **503**, 513 (2003).
178 [19] V. D. Burkert *et al.* (*CLAS Collaboration*), NIM A **959**, 163419 (2020).